LA-UR- 09-06175

Approved for public release; distribution is unlimited.

Title:	Runoff simulations from the Greenland Ice Sheet at Kangerlussuaq from 2006/2007 to 2007/08. West Greenland
Author(s):	Sebastian H. Mernild, LANL; Bent Hasholt, University of Copenhagen; Michiel van den Broeke, Utrecht University; and Glen Liston, Colorado State University.
Intended for:	Water Resources Research

Los Alamos
NATIONAL LABORATORY
EST. 1943

Form 836 (7/06)

Runoff simulations from the Greenland Ice Sheet at Kangerlussuaq from 2006/07 to 2007/08, West Greenland

SEBASTIAN H. MERNILD

Climate, Ocean, and Sea Ice Modeling Group, Computational Physics and Methods, Los Alamos National Laboratory, New Mexico, USA, and International Arctic Research Center and Water & Environmental Research Center, University f Alaska Fairbanks, Alaska, USA

BENT HASHOLT

Department of Geography and Geology, University of Copenhagen, DENMARK

MICHIEL van den BROEKE

Institute for Marine and Atmospheric Research, Utrecht University, HOLLAND

GLEN E. LISTON

Cooperative Institute for Research in the Atmosphere, Colorado State University, Colorado, USA

Submitted 6 August 2009 to Water Resources Research

Corresponding author address:
Dr. Sebastian H. Mernild
Climate, Ocean, and Sea Ice Modeling Group, Computational Physics and Methods (CCS-2)
Los Alamos National Laboratory,
Los Alamos, New Mexico 87545
USA
E-mail: mernild@lanl.gov

Abstract

This study focuses on runoff from a large sector of the Greenland Ice Sheet (GrIS)—the Kangerlussuaq drainage area, West Greenland—for the runoff observation period 2006/07 to 2007/08. SnowModel, a state-of-the-art snow-evolution modeling system, was used to simulate winter accumulation and summer ablation processes, including runoff. Independent in situ end-of-winter snow depth and high-resolution runoff observations were used for validation of simulated accumulation and ablation processes. Runoff was modeled on both daily and hourly time steps, filling a data gap of runoff exiting part of the GrIS. Using hourly meteorological driving data instead of smoothed daily-averaged data produced more realistic meteorological conditions in relation to snow and melt threshold surface processes, and produced 6–17% higher annual cumulative runoff. The simulated runoff series yielded useful insights into the present conditions of inter-seasonal and inter-annual variability of Kangerlussuaq runoff, and provided an acceptable degree of agreement between simulated and observed runoff. The simulated spatial runoff distributions, in some areas of the GrIS terminus, were as high as 2,750 mm w.eq. of runoff for 2006/07, while only 900 mm w.eq was simulated for 2007/08. The simulated total runoff from Kangerlussuaq was 1.9 km^3 for 2006/07 and 1.2 km^3 for 2007/08, indicating a reduction of 35–40% caused by the climate conditions and changes in the GrIS freshwater storage. The reduction in runoff from 2006/07 to 2007/08 occurred simultaneously with the reduction in the overall pattern of satellite-derived GrIS surface melt from 2007 to 2008.

KEY WORDS: Freshwater, Greenland Ice Sheet, Kangerlussuaq, observations, runoff, SnowModel, Søndre Strømfjord

1. Introduction

The Greenland Ice Sheet (GrIS) is the Northern Hemisphere's largest terrestrial permanent ice- and snow-covered area. The GrIS is a reservoir of water that is highly sensitive to changes in climate [e.g., *Box et al.*, 2006; *Fettweis*, 2007; *Hanna et al.*, 2007, 2008; *Mernild et al.*, 2008a, 2009b]. It is essential to assess the impact of climate change on the GrIS, since the temperature rise at higher northern latitudes strongly correlates with global warming, and is confirmed to have increased at almost twice the global average rate in the past 100 years [*IPCC*, 2007]. A response to altered climate has already been observed on the GrIS, manifested by an accelerating surface melt extent, thinning along the periphery, mass loss, and freshwater runoff [e.g., *Krabill et al.*, 2000, 2004; *Janssens and Huybrechts*, 2000; *Zwally et al.*, 2002; *Johannessen et al.*, 2005; *Box et al.*, 2006; *Fettweis*, 2007; *Ettema et al.*, 2009; *Hanna et al.*, 2009; *Mernild et al.*, 2009a, 2009b; *Richardson et al.*, 2009].

In spite of the need for information about GrIS freshwater runoff, only a few high-resolution runoff observations are available to fill the gap in hydrologic measurements of water exiting the GrIS [*Mernild et al.*, 2008d; *Mernild and Hasholt,* 2009; *Hasholt and Mernild*, 2009]. This measurement gap is particularly noticeable in the context of varying ice sheet surface melt and temporary seasonal runoff storage buildup (delay) and storage release by internal deformation of the GrIS drainage system [e.g., *Stenborg*, 1970; *Jansson et al.*, 2003]. Such observations are of considerable interest for estimating the impact of runoff on the arctic marine ecosystem and for obtaining knowledge about the onset, duration, and intensity of runoff and its hydrological response during the year. High-resolution runoff observations are further useful as runoff model validation, for example, before modeling ungauged GrIS sub-basin runoff, for simulating freshwater resource availability, for defining controls on global eustatic sea level rise, and for quantifying runoff affects on modifying ocean salinity [e.g., *Dowdeswell et al.*, 1997; *ACIA*, 2005; *IPCC*, 2007]. Such high-resolution runoff observations have been maintained at Kangerlussuaq (Søndre Strømfjord), West Greenland, since June 2007, providing information on stage and runoff from a sector of the GrIS [*Mernild et al.*, 2008d; *Mernild and Hasholt*, 2009]. Kangerlussuaq is one of the best locations for observing GrIS runoff due to the well-defined, stable bedrock cross sections at the catchment outlet [*Mernild et al.*, 2008d]. Most other river outlets in Greenland have braided channels with unstable banks, making accurate runoff monitoring nearly impossible.

To model the impact of seasonally changing processes on the GrIS surface hydrological cycle—surface mass balance (SMB)—different seasonal processes need to be accounted for and understood. Throughout the GrIS, much of the winter precipitation falls as a solid, under windy conditions. As winter progresses, the solid precipitation accumulates and is frequently redistributed during blowing snow events. A further consequence of this blowing snow is that significant portions (10–50%) of snow cover can be returned to the atmosphere by sublimation of wind-borne snow particles [*Liston and Sturm*, 1998, 2002; *Essery et al.*, 1999; *Pomeroy and Essery*, 1999; *Mernild et al.*, 2008a]. As spring and summer progress, the variation, duration, and intensity of snow and glacier melt increase in response to the impact in weather and climate (e.g., insolation, temperature inversions, and wind speed) and surface characteristics (e.g., albedo, roughness). The moisture in this system also changes phase (solid, liquid, and vapor) throughout the year as part of various physical processes and in response to the available surface and snowpack energy fluxes. It is essential to account for the role of snowpack meltwater retention; the overall GrIS runoff would be overestimated by approximately 20–30% if no model retention/refreezing routines were included in model simulations [e.g., *Hanna et al.*, 2002, 2005, 2008; *Mernild et al.*, 2008a]. These seasonally changing processes directly impact the seasonal evolution (mass fluxes) of the GrIS surface hydrological cycle, including the evolution of the internal drainage system and the influx of freshwater to the ocean (e.g., van de Wal et al. 2008).

Modeling the GrIS SMB, including surface runoff, is relatively well understood and documented in numerical models [e.g., *Box et al.*, 2006; *Fettweis*, 2007; *Hanna et al.*, 2007; *Ettema et al.*, 2009; *Mernild et al.*, 2009a, 2009b]. Efforts to model the GrIS mass balance, its dynamic processes, changes, and internal drainage related to runoff contribution to the global eustatic sea level rise, still suffer from important uncertainties and limitations [*Parizek and Alley*, 2004; *Lemke at al.*, 2007; *van den Broeke et al.*, 2008]. The mechanisms that link climate, the GrIS SMB, ice dynamics, and internal ice sheet hydrology (e.g., routing of water: meltwater and liquid precipitation through glacier ice, transforming the input contributions into a runoff hydrograph at the ice sheet terminus based on seasonal changes in hydrological response and delay) are poorly understood. Current numerical ice sheet models do not simulate these changes realistically [*Nick et al.*, 2009]. In spite of this. there is growing recognition that accurate representations of SMB and internal drainage are essential to realistically assess the impact of climate changes on the GrIS. Simple and crude conceptual models have described glaciers as

porous media and as a system of reservoirs, with different storage properties [e.g., *Campbell and Rasmussen*, 1973; *Hock and Hoetzli*, 1997; *Jansson et al.*, 2003]. With the purpose of simulating runoff from glacierized basins, however, these models omit many of the key physical processes.

This study attempts to improve our quantitative understanding of the Kangerlussuaq freshwater runoff and changes—the drainage of a large sector of the GrIS. The goal of this study was to apply a well-tested, state-of-the-art surface modeling system—SnowModel [*Liston and Elder* 2006a; *Mernild et al.*, 2006a; *Liston et al.*, 2007]—to the Kangerlussuaq region, West Greenland. SnowModel routines were compared to independent in situ field snow depth and catchment-outlet runoff observations. We performed model simulations both on daily and hourly time steps for the 2-year runoff observation period (2006/07 through 2007/08) for the Kangerlussuaq drainage area. Our objectives were (1) to simulate winter processes related to snow accumulation, snow redistribution by wind, and snow sublimation; (2) to simulate runoff from the drainage area based on meteorological input data from both on and outside the GrIS, and outside the GrIS alone; (3) to compare modeled runoff outputs with available independent observational data sets; (4) to show the difference in runoff based on daily and hourly time steps; and (5) to generate daily and hourly time series and area-distributed runoff fluxes from the seasonal snowpack and the exposed glacier surface to be used as meltwater inputs to hydrological routing models.

2. Study area

a. Physical settings, meteorological stations, and climate

The Kangerlussuaq drainage area (6,279 km^2) is located on the west coast of Greenland (67°N latitude; 50°W longitude) (Figure 1a), and provides drainage for a large sector of the GrIS. The runoff measurement site is located approximately 35 km downstream from the GrIS terminus, near the town Kangerlussuaq (Søndre Strømfjord) at the bottom of the Kangerlussuaq Fjord. This stream gauge location is one of the best available for observing GrIS runoff due to the well-defined stable bedrock cross section (braided channels with unstable banks characterize most other river outlets in Greenland, making accurate runoff monitoring almost impossible).

The simulated Kangerlussuaq region (21,248 km^2) (Figure 1) covers the western part of the GrIS (14,776 km^2) and 6,472 km^2 of the proglacial landscape. The simulation area is characterized by elevations that range to ~1,800 m a.s.l. (Figure 1b). The land cover is dominated

by glacier ice in the upper parts of the terrain, and bare bedrock/vegetation and river valleys in the lower parts (Figure 1c).

Four meteorological stations are located within the simulation domain, and three of them on the GrIS (Figure 1c). Station Kangerlussuaq (hereafter referred to as Station K) (67°01′N, 50°42′W; 50 m a.s.l.; a standard synoptic Danish Meteorological Institute [DMI] WMO meteorological station) is located within the town of Kangerlussuaq. Station K is representative of proglacial conditions, influenced by the Kangerlussuaq Fjord. Station S5 (67°06′N, 50°07′W; 490 m a.s.l.), S6 (67°05′N, 49°23′W; 1,020 m a.s.l.), and S9 (67°03′N, 48°14′W; 1,520 m a.s.l.) are all part of the K-transect located on the ice sheet, and representative of GrIS conditions (for further information about the K-transect stations, see, e.g., *van de Wal et al.* [2005] and *van den Broeke et al.* [2008a, 2008b, 2008c]). The mean equilibrium line altitude (ELA; defined as the elevation where the net mass balance is zero) is ~1,530 m a.s.l., located near Station S9 [*van de Wal et al.*, 2005; *van den Broeke et al.*, 2008c].

The Kangerlussuaq region is considered Low Arctic according to *Born and Böcher* [2001]. The SnowModel simulated mean annual air temperature for the simulation domain (2003–2007) is -7.7°C. Mean annual relative humidity is 64%, and mean annual wind speed is 4.8 m s^{-1}. The corrected mean total annual precipitation (TAP) for the region is 419 mm w.eq. y^{-1} [corrected after *Allerup et al.*, 1998, 2000; *Mernild et al.*, 2007, 2008a].

3. Water balance components

Throughout the year, different surface processes (snow accumulation, snow redistribution, blowing-snow sublimation, surface evaporation, and melting) on snow and glacier ice affect the surface glacier mass balance and the high-latitude water balance, including runoff. The yearly water balance equation for a glacier is described by

$$P - (E+SU) - R \pm \Delta S = 0 \pm \eta \quad (1)$$

where P is the precipitation input from snow and rain (and possible condensation), E is evaporation, SU is sublimation (including blowing-snow sublimation), R is runoff, and ΔS is change in storage (ΔS is also referred to as the SMB) from changes in glacier ice storage and snowpack storage. Glacier storage also includes changes in supraglacial storage (lakes, ponds,

channels, etc.), englacier storage (ponds and the water table), and subglacier storage (cavities and lakes); glacier storage components were not accounted for in this study. Here, η is the water balance discrepancy (error). The error term should be 0 (or small) if the major components (P, E, SU, R, and ΔS) have been determined accurately.

4. SnowModel

a. SnowModel description

SnowModel [*Liston and Elder*, 2006a] is a spatially distributed meteorological and snowpack evolution modeling system. It is made up of five submodels: MicroMet (a quasi–physically-based meteorological distribution model) defines the meteorological forcing conditions [*Liston and Elder*, 2006b]. EnBal calculates the surface energy exchanges, including melt [*Liston*, 1995; *Liston et al.*, 1999]. SnowPack simulates heat and mass transfer processes, and snow depth and water equivalent evolution [*Liston and Hall*, 1995]. SnowTran-3D is a blowing-snow model that accounts for snow redistribution by wind [*Liston and Sturm*, 1998, 2002; *Liston et al.*, 2007]. SnowModel also includes a snow data assimilation submodel (SnowAssim [*Liston and Hiemstra,* 2008]) that can be used to assimilate available snow measurements to create simulated snow distributions that closely match observed distributions when and where they occur [*Liston et al.*, 2008]. SnowModel was originally developed for glacier-free landscapes. For glacier SMB studies in Greenland, SnowModel was modified to simulate (1) glacier-ice melt after winter snow accumulation had ablated [*Mernild et al.*, 2006a, 2007]; (2) the influence of air temperature inversions on snowmelt and glacier SMB simulations where radiosonde data is present [*Mernild and Liston*, 2009]; and (3) variable snow albedo as the snow ages and precipitation occurs [*Mernild et al.*, 2009c]. For this study, routines for temperature inversion were not included because of the lack of available radiosonde data in the area. SnowModel is a surface energy- and mass-balance model that simulates the first-order effects of variations and changes in atmospheric forcing and other climate features; it does not include glacio-hydro-dynamic and glacio-sliding routines.

1) MICROMET

MicroMet is a quasi–physically-based meteorological distribution model [*Liston and Elder*, 2006b] specifically designed to produce the high-resolution meteorological forcing

distributions (air temperature, relative humidity, wind speed, wind direction, precipitation, solar and long-wave radiation, and surface pressure) required to run spatially distributed terrestrial models over a wide range of landscapes. MicroMet uses elevation-related interpolations to modify air temperature, humidity, and precipitation following *Kunkel* [1989], *Walcek* [1994], *Dodson and Marks* [1997], and *Liston et al.* [1999]. Temperature and humidity distributions are defined to be compatible with observed lapse rates. Wind flow in complex topography is simulated following *Ryan* [1977] and *Liston and Sturm* [1998]. Solar radiation variations are calculated using elevation, slope, and aspect relationships [*Pielke*, 2002]. Incoming long-wave radiation is calculated while taking into account cloud cover and elevation-related variations following *Iziomon et al.* [2003]. Precipitation is distributed following *Thornton et al.* [1997]. In addition, any data from more than one location at any given time are spatially interpolated over the domain using a Gaussian distance-dependent weighting function, and interpolated to the model grid using the Barnes objective analysis scheme [*Barnes,* 1964, 1973; *Koch et al.,* 1983]. *Liston and Elder* [2006b], *Liston et al.* [2007], *Mernild et al.* [2008a], and *Mernild and Liston* [2009] have performed a rigorous validation of MicroMet using various observational data sets, data denial, and geographic domains. Further, MicroMet has been used to distribute observed and modeled meteorological variables over a wide variety of snow and glacier landscapes in the United States (Colorado [*Greene et al.,* 1999], Wyoming [*Hiemstra et al.*, 2002, 2006], Idaho [*Prasad et al.*, 2001], and Arctic Alaska [*Liston et al.* 2002, 2007; *Liston and Sturm*, 1998, 2002]. Other locations where MicroMet has been used include Norway (Svalbard and central Norway) [*Bruland et al.*, 2004]; East Greenland [*Mernild et al.*, 2006a, 2007, 2008c; *Mernild and Liston*, 2009]; the Greenland Ice Sheet [*Mernild et al.*, 2008a, 2008b, 2009a, 2009b, 2009c]; and near-coastal Antarctica [*Liston et al.*, 1999; *Liston and Winther*, 2005].

2) ENBAL

EnBal performs standard surface energy-balance calculations [*Liston*, 1995; *Liston et al.*, 1999]. This component simulates surface (skin) temperatures and energy and moisture fluxes in response to observed and/or modeled near-surface atmospheric conditions provided by MicroMet. Surface latent and sensible heat flux and snowmelt calculations are made using a surface energy-balance model of the form:

$$(1 - \alpha)\, Q_{si} + Q_{li} + Q_{le} + Q_h + Q_e + Q_c = Q_m, \quad (2)$$

where Q_{si} is the solar radiation reaching the earth's surface, Q_{li} is the incoming long-wave radiation, Q_{le} is the emitted long-wave radiation, Q_h is the turbulent exchange of sensible heat, Q_e is the turbulent exchange of latent heat, Q_c is the conductive energy transport, Q_m is the energy flux available for melt, and α is the surface albedo. Details of each term in Equation 2 and the model solution are available in *Liston* [1995] and *Liston et al.* [1999]. In the presence of snow or glacier ice, surface temperatures greater than 0°C indicate that energy is available for melting. This energy is computed by fixing the surface temperature at 0°C and solving Equation 2 for Q_m. Energy transports toward the surface are defined to be positive.

3) SNOWPACK

SnowPack is a single-layer, snowpack evolution and runoff/retention model that describes snowpack changes in response to precipitation and melt fluxes defined by MicroMet and EnBal [*Liston and Hall*, 1995; *Liston and Elder*, 2006a]. Its formulation closely follows *Anderson* [1976]. In SnowPack, the density changes with time in response to snow temperature and weight of overlying snow [*Liston and Elder*, 2006a]. A second density modifying process results from snow melting. The melted snow reduces the snow depth and percolates through the snowpack. If snow temperature is below freezing, any percolating/liquid water refreezes and is stored in the snow (in the "pores") as internal refreezing. When saturated snow density is reached, assumed to be 550 kg m^{-3} [*Liston and Hall*, 1995], actual runoff occurs. This provides a method to account for heat and mass transfer processes, such as snowpack ripening, during spring melt. The density of new snow from additional accumulation is defined following *Anderson* [1976] and *Liston and Hall* [1995]. Static-surface (non-blowing snow) sublimation calculated in EnBal is used to adjust the snowpack depth; blowing-snow sublimation is calculated in SnowTran-3D [*Liston and Elder*, 2006a].

4) SNOWTRAN-3D

SnowTran-3D [*Liston and Sturm*, 1998; *Liston et al.*, 2007] is a three-dimensional submodel that simulates snow depth evolution (deposition and erosion) resulting from windblown snow, based on a mass balance equation that describes the temporal variation of

snow depth at each grid cell within the simulation domain. The primary components of SnowTran-3D are a wind-flow forcing field, a wind shear stress on the surface, snow transport by saltation, snow transport by turbulent suspension, sublimation of saltating and suspended snow, and accumulation and erosion at the snow's surface [*Liston and Sturm*, 2002]. Simulated transport and blowing-snow sublimation processes are influenced by the interactions among available snow, topography, and atmospheric conditions [*Liston and Sturm*, 1998]. SnowTran-3D simulates snow depth evolution and then uses the snow density simulated by SnowPack to convert it to the more hydrologically significant snow water equivalent (SWE) depth. Deposition and erosion, which lead to changes in snow depth (Equation 3), are the result of changes in horizontal mass transport rates of saltation, Q_{salt} (kg m^{-1} s^{-1}), changes in horizontal mass transport rates of turbulent suspended snow, Q_{turb} (kg m^{-1} s^{-1}), sublimation of transported snow particles, Q_v (kg m^{-2} s^{-1}), and the water equivalent precipitation rate, P (m s^{-1}). Combined, the time rate of change in snow depth, ζ (m), is

$$\frac{d(\rho_s \zeta)}{dt} = \rho_w P - \left(\frac{dQ_{salt}}{dx} + \frac{dQ_{turb}}{dx} + \frac{dQ_{salt}}{dy} + \frac{dQ_{turb}}{dy}\right) + Q_v \qquad (3)$$

where t (s) is time; x (m) and y (m) are the horizontal coordinates in the west–east and south–north directions, respectively; and ρ_s and ρ_w (kg m^{-3}) are snow and water density, respectively. At each time step, Equation 3 is solved for each individual grid cell within the domain, and is coupled to the neighboring cells through the spatial derivatives (*d/dx, d/dy*). SnowTran-3D simulations have previously been compared against observations in glacier and glacier-free alpine, Arctic, and Antarctic landscapes [*Greene et al.*, 1999; *Liston et al.*, 2000, 2007; *Prasad et al.*, 2001; *Hiemstra et al.*, 2002, 2006; *Liston and Sturm*, 2002; *Bruland et al.*, 2004; *Mernild et al.*, 2006a, 2008a, 2008b, 2009a, 2009b, 2009c].

5) SNOWASSIM

The SnowModel snow data assimilation scheme (SnowAssim [*Liston and Hiemstra*, 2008]) is designed to push the model snow-distribution simulations toward observed snow depths, when and where such observations exist. This is done by adjusting the precipitation inputs in order to match the observed snow on the ground. The data assimilation scheme is

consistent with optimal interpolation approaches, where the differences between observed and modeled snow values constrain modeled outputs. The calculated precipitation corrections are applied backwards in time to create improved fields prior to the assimilated observations. Thus, one of the values of the scheme is improved simulation of snow-related distributions throughout the entire snow season, even when observations are only available sporadically or late in the accumulation and/or ablation periods.

b. SnowModel input

To solve its system of equations, SnowModel requires spatially distributed fields of topography and land cover, and temporally distributed point meteorological data (air temperature, relative humidity, wind speed, wind direction, and precipitation) obtained from meteorological stations located within the simulation domain. For this study, high-resolution data are obtained from four meteorological stations: three stations (S5, S6, and S9) from the K-transect, and one standard synoptic DMI WMO operated station (Station K) (Figure 1c, Table 1). The simulations span the two-year runoff observation period 1 September 2006 through 31 August 2008, and were performed on both daily and hourly time steps. For 2006/07, input data from (1) Station K, S5, S6, and S9, and (2) Station K alone were used. For 2007/08, data from Station K were only used (data from S5, S6, and S9 were not available for 2007/08).

Mean monthly lapse rates (September 2003 through August 2007), based on air temperature observations from the Station S5, S6, and S9 transect, were used as model input (Table 2). A minimum monthly temperature lapse rate of -8.6°C km^{-1} occurred in October, and a maximum of -4.6°C km^{-1} occurred in July. The mean annual Kangerlussuaq GrIS lapse rate of -6.7°C km^{-1} is consistent with average western GrIS lapse rates of -7.8°C km^{-1} [*Steffen and Box*, 2001], and average Jakobshavn and GrIS values of -7.1 and -7.5°C km^{-1}, respectively [*Mernild et al.*, 2009b, 2009c].

Across the Arctic it is well known that precipitation gauges significantly underestimate solid precipitation because of aerodynamic errors at the gauging station, especially under windy and cold conditions [e.g., *Yang et al.*, 1999; *Liston and Sturm*, 2002, 2004; *Serreze and Barry*, 2005). Solid and liquid precipitation measurements at the DMI meteorological station (Figure 1c, Table 1) were calculated from Helman–Nipher shield observations corrected according to *Allerup et al.* [1998, 2000].

Greenland topographic data for model simulations were provided by *Bamber et al.* [2001] who applied "correction" elevations derived by satellite imagery to an existing radar-altimetry digital elevation model (DEM). The image-derived correction was determined from a high-resolution (625 m) grid of slopes inferred from the regional slope-to-brightness relationship of 44 AVHRR images covering all of Greenland [*Scambos and Haran*, 2002]. For the model simulations presented herein, this DEM was aggregated to a 500 m grid-cell increment and clipped to yield a 128 by 166 km simulation domain (21,248 km^2; the Kangerlussuaq region) (Figure 1b). The GrIS ice terminus was estimated using satellite images (Google Earth, Image 2009). Each grid cell within the domains was assigned a USGS Land Use/Land Cover System class according to the North American Land Cover Characteristics Database, Version 2.0 (available on-line at [http://edcdaac.usgs.gov/glcc/na_int.html] from the USGS EROS Data Center's Distributed Active Archive Center, Sioux Falls, South Dakota, USA). The snow-holding depth in SnowModel (the snow depth that must be exceeded before snow can be transported by wind) was assumed constant (Table 3). A variable snow albedo was calculated using *Douville et al.* [1995] and *Strack et al.* [2004], gradually decreasing the albedo from 0.8 to a minimum of 0.5 as the snow ages [for further information, see *Mernild et al.*, 2009c]. When the snow is ablated, GrIS surface ice conditions are used. Albedo was assumed to be a constant 0.4 for ice; however, other studies have noted the GrIS ablation area is characterized by a lower albedo on the margin that increases toward the ELA, where a veneer of ice and snow dominate the surface [*Boggild et al.*, 2006]. Emergence and melting of old ice in the ablation area create surface layers of dust (black carbon particles) that originally were deposited with snowfall higher on the ice sheet. This debris cover is often augmented by locally derived windblown sediment. Particles on or melting into the ice change the area-average albedo, increasing melt. User-defined constants for SnowModel are shown in Table 3 [for parameter definitions, see *Liston and Sturm*, 1998, 2002].

c. SnowModel calibration, validation, and uncertainty

SnowModel was chosen for this study because of its robustness and ease of implementation over new simulation domains. This model demands rather limited input data, an important consideration in areas like Kangerlussuaq for which data are sparse. To assess the general performance of the SnowModel-simulated distributed meteorological data and snow

evolution, snow and ice surface melt, and glacier net mass balance and snow and ice processes, simulated values have been tested against independent observations. SnowModel/MicroMet distributed meteorological data have been compared against independent Greenland meteorological station data both on and outside the GrIS, indicating respectable (84–87% variance for air temperature, 49–55% for wind speed, 49–69% for precipitation, and 48–63% for relative humidity) representations of meteorological conditions [for further information, see *Mernild et al.*, 2008a; *Mernild and Liston*, 2009]. Few validation observations for in situ snow evolution, snow and ice surface melt, and glacier net mass balance are available in Greenland. Therefore, SnowModel accumulation and ablation routines were tested qualitatively (by visual inspection) and quantitatively (cumulative values and linear regression) using independent in situ observations on snow pit depths; glacier winter, summer, and net mass balances; depletion curves; photographic time lapses; and satellite images also from in and outside the GrIS [*Mernild et al.*, 2006a, 2006b, 2007, 2008a, 2008b, 2009a, 2009b 2009c; *Mernild and Liston*, 2009]. In these studies, a comparison performed between simulated and observed values indicates a 7% maximum difference between modeled and observed snow depths, glacier mass balance, and snow cover extent.

To assess the winter and summer model performance for this Kangerlussuaq study, the end-of-winter (31 May; recognized as the end of the accumulation period) simulated snow depth was compared with Station S9 observed snow depth, and the simulated cumulative summer (June through August) runoff was compared with observed catchment-outlet runoff entering directly into the Kangerlussuaq Fjord (Figure 1c). The Station S9 snow depth was measured 31 May, and used to verify and adjust the SnowModel simulated snow depth (Table 4). The simulated snow depth was on average overestimated by ~50% (400 mm w.eq.) for 2003/04–2006/07, and up to ~70% (620 mm w.eq.) for 2003/04 (Table 4). The iterative precipitation adjustment routines yield a simulated Station S9 snow depth on 31 May that was within 1% of the observed snow depth (Table 4) [for further information, see *Mernild et al.*, 2006a; *Liston and Hiemstra*, 2008]. The catchment outlet runoff was observed for the 2007 and 2008 runoff seasons [*Mernild et al.*, 2008d; *Mernild and Hasholt*, 2009]. Stage and discharge measurements were used to develop a stage-discharge relationship (R^2=0.91) and to convert the stage measurements into a river runoff time series. The relationships are expected to have an accuracy of 10–15% [*Mernild and Hasholt*, 2009]. For 2007, the cumulative simulated runoff differs ~90% from observed values

(Table 5; simulations based on input data from all four meteorological stations). After runoff adjustment, the difference in simulated and observed runoff was within 1% for 2007 (Table 5; Figure 2a). In Figure 2b, daily time series of modeled and observed runoff for 2007 are illustrated, showing an acceptable seasonal variability in runoff, with R^2-values (the explained variance) of 0.44 (daily time step) and 0.58 (5-day running average). The choice of the 5-day running average is due to the highest R^2-value: 2-day running average (R^2=0.46), 3-day (0.48), and 4-day (0.55), and 6-day (0.57) (Figure 2c). On an hourly basis, the 2007 R^2-value for the 5-day/120-hour running average was 0.57 (Figure 4c).

Since meteorological data only were available from Station K (representative of proglacial conditions) for the 2008 simulations, the 2007 runoff was re-simulated based on Station K input data only. This simulation overestimates the 2007 observed cumulative runoff by ~270% (Table 5, Figure 3a), due, for example, to the average higher temperature conditions in the proglacial landscape, than on the GrIS. Station K experiences quite different temperatures compared to the GrIS. The summer days can be warm, since the tundra is relatively dark and dry. In contrast, the winters at Station K are relatively colder than over the GrIS, because the absence of persistent katabatic winds allows for the formation of a strong temperature inversion in the valleys. This ~270% overestimation was used for adjustment of the 2008 simulated runoff, which indicates a difference within ~10% of the observed 2008 cumulative runoff (Table 5). For the 2008 simulated and observed time series, the R^2-values are 0.43, 0.49, and 0.55 for the daily simulations based on daily values, 5-day running average values, and for hourly simulations performed on 120-hour (5-day) running average values, respectively (Figures 3c, 4d).

It appears that our choice of a simple adjusted methodology that provides estimates of the Kangerlussuaq cumulative runoff agree well with observed values. Nevertheless, it is important to keep in mind the limitation for SnowModel results (1) when tested against sparse observations and (2) when model uncertainties are largely determined by processes not yet represented by standard routines in the modeling system. Such processes would include, for example, routines for simulating changes in GrIS area, size, and surface elevation according to glacier dynamic and sliding processes. Runoff from geothermal heating/melting was omitted for the calculations. Further, changes in the GrIS storage, based on supraglacial, englacial, subglacial, and proglacial storage, internal meltwater routing, and the evolution of the internal runoff drainage system are not calculated in SnowModel, even though they might influence runoff.

5. Results and discussion

Blowing snow, snowmelt, and ice-melt are threshold processes that may not be accurately represented by daily time step simulations, since daily-averaged atmospheric-forcing variables, in contrast to hourly data, smoothed the meteorological driving data. In Figures 2b, 3b, 4a, and 4b, daily and hourly time step modeled Kangerlussuaq runoff for the 2007 and 2008 runoff observation period (June through August) is illustrated, indicating (1) fewer variations and fluctuations in daily modeled runoff values, compared with hourly modeled values; and (2) more smoothed daily runoff values compared with direct runoff observations (Figures 4c and 4d). Due to the smoothed trend in daily time-step simulated runoff, daily simulations indicated a lower cumulative runoff of ~6–14% ($0.089–0.237\times10^9$ m^3), than hourly time step simulated runoff for the observation period (Table 6). For the entire 2006/07 and 2007/08 runoff period (September through August), the trend is similar, but more pronounced, since a difference of ~9–17% ($0.109–0.298\times10^9$ m^3) occurred in cumulative runoff between daily and hourly simulations (Table 6). A similar time step difference is illustrated in modeled runoff originating from the glacier ice on the GrIS. For 2006/07, the modeled runoff (based on a daily time step) indicates that ~58% (1.011×10^9 m^3) of the runoff originated from glacier ice. Similar simulations (hourly based) indicate that ~64% (1.326×10^9 m^3) of the runoff originated from the glacier ice. A similar trend is present for 2007/08, but is less pronounced, since only ~54% (0.627×10^9 m^3) and ~55% (0.694×10^9 m^3) of the runoff originated from the glacier ice (Table 6). The use of less smoothed meteorological input data—hourly data instead of daily-averaged—indicates more realistic meteorological conditions related to threshold surface processes and a relatively higher cumulative runoff: a difference illustrated to be between 6–17%.

A division of the 2007 and 2008 daily and hourly observed and simulated runoff time series (June through August) is illustrated in Figures 2b, 3b, 4c, and 4d. This division is due to the temporary seasonal GrIS storage buildup (delay) and release of runoff mainly by internal deformation of the drainage system. Time series are divided after *Stenborg* [1970] into sub-seasonal periods: Period I, II, and III. Period I is characterized by simulated surface runoff exceeding the observed outlet runoff (indicating temporary GrIS storage buildup). Period II is where simulated runoff almost equals observed runoff. Period III is where observed outlet runoff exceeds simulated surface runoff (indicating storage release). For Kangerlussuaq (daily time

step), Period I is in the beginning of the runoff season until the end of June; Period II, from the end of June to the end of July; and Period III, in the end of the runoff season from the end of July (Figures 2b and 3b). For hourly time step, the division of the time series seems more variable (Figure 4c and 4d). The seasonal delay—the temporary storage buildup and release—of runoff from Kangerlussuaq is typical for glacierized basins: a runoff delay due to changes in hydrological response related to the GrIS drainage properties.

For 2006/07, the simulated cumulative runoff was 1.76×10^9 m^3 (1.76 km^3) (daily time step), and 2.06×10^9 m^3 (2.06 km^3) (hourly time step), averaging ~1.9 km^3 (Table 6, Figure 2d). For 2007/08, the runoff was 1.15×10^9 m^3 (1.15 km^3) and 1.26×10^9 m^3 (1.26 km^3), averaging ~1.2 km^3 (Figure 3d, Table 6), indicating a reduction in runoff of 35–40% from 2006/07 to 2007/08. The specific runoff from the modeled area was 20.9 L s^{-1} km^{-2} y^{-1} and 14.0 L s^{-1} km^{-2} y^{-1} for 2006/07 and 2007/08, respectively. A specific runoff 2–3 times the average specific runoff of 6.9(±1.2) L s^{-1} km^{-2} y^{-1} for the GrIS for the period 1995–2007 [*Mernild et al.*, 2009b] indicates that Kangerlussuaq runoff is above the spatial average specific runoff for the GrIS.

The reduction in Kangerlussuaq runoff of 35–40% from 2006/07 to 2007/08 appears to follow the overall variation in the satellite-derived GrIS surface melt for 2007 and 2008. From 2007 to 2008, the GrIS melting area decreased ~25% [*Richardson et al.*, 2009]. Melting reduction in the broad GrIS perspective seems to occur simultaneously with reduction in the local Kangerlussuaq runoff. Therefore, it is expected that the reduction in annual runoff of 35–40% might be explained by variations in local meteorological conditions. This explanation is based on meteorological records (June through August) from Station K (the only station used since data from Station S5, S6, and S6 were only available for 2007/08), which show a surprisingly similar mean summer temperature for the two years of 10.5°C and 10.3°C, but a more pronounced difference in precipitation. The corrected precipitation (June through August) was 119 mm w.eq. for 2007, but only 72 mm w.eq. for 2008, indicates a difference of 47 mm w.eq. Since Station K data are recorded at Kangerlussuaq (in the proglacial area), not on the GrIS, one must be careful about conclusively stating the reason for the 35–40% reduction in cumulative runoff, as there is a different climate and variations on and outside the GrIS. Obviously, it is possible that the meteorological data from Station K are not representative of the conditions on the GrIS. However, one explanation for the annual runoff difference could be that there are year-to-year changes in the GrIS freshwater storage (see Equation 1). The higher

cumulative discharge in 2007 could be caused by a release of water stored on the GrIS surface, internally, or in ice-dammed lakes, a hypothesis that may be partly supported by observed jökulhlaups [*Mernild et al.*, 2008d; *Hasholt and Mernild*, 2009] (Figures 4c and 4d). Figures 4c and 4d include a short-lived jökulhlaup event in 2007 and 2008, both of which occurred on 31 August. Both the 2007 and 2008 events occurred after 4 days with a mean daily air temperature of 11–12°C. In 2007, the sharp drainage increase was preceded by a period of high precipitation with 33 mm w.eq., whereas in 2008, conditions were dry (3 mm w.eq.) before the drainage took place [*Mernild et al.*, 2008d; *Mernild and Hasholt*, 2009]. This dissimilarity probably indicates initiating the jökulhlaups result from different weaknesses in the sub-GrIS internal drainage system combined with relatively high mean daily air temperatures. While it is clear that such releases of water occur on the GrIS and certainly influence general runoff and peak event timing and magnitudes, SnowModel does not account for such sudden releases of water storage.

In Figures 6a and 6b, the 2006/07 and 2007/08 daily and hourly modeled spatial-runoff variation for the Kangerlussuaq region is illustrated. Our analysis of the spatial runoff distribution shows that in some areas of the GrIS terminus, for example, at the Russell Glacier (near Station S5), as much as ~2,750 mm w.eq. of runoff was simulated for 2006/07, while only ~900 mm w.eq was simulated for 2007/08 (both for daily and hourly time steps) (Figures 6a and 6b). The annual runoff discrepancy between the runoff and non-runoff boundaries is located around 71–89 km (2006/07) and 67–84 km (2007/08) (whether daily or hourly time step are used) from the Russell Glacier terminus and further inland, at approximately 1,400–1,550 m a.s.l. and 1,375–1,500 m a.s.l., respectively (Figures 6a and 6b).

Figures 2a, 3a, and 5 illustrate the annual time series for daily and hourly surface runoff production from both snow cover and glacier ice throughout winter and summer from 2006/07 and 2007/08. Figures 6a and 6b present the spatial distribution of cumulative runoff for the same periods. During winter (September/October through May), no runoff events where simulated (either on a daily or hourly basis) for the Kangerlussuaq drainage area. The first day for annual modeled runoff occurred in the end of May 2007 and in mid-May 2008, and up to approximately one week before, due to the hourly simulations (Figure 5). Visual observations indicate that outlet runoff normally starts around mid/late April [*Hasholt and Mernild*, 2009], approximately 2–3 weeks before simulated runoff, and stops in late September to mid-October, which is in accordance with simulated values.

In the early melt period (April and May), surface melt was mainly controlled by snowmelt, whereas later in the season (mid-July and August), when the snow cover was largely gone, surface melt was dominated by glacier-ice melt. When surface melting is simulated by SnowModel, meltwater is assumed to run as "runoff" instantaneously when the surface consists of glacier ice. When snow cover is present, the SnowPack runoff routines take retention and internal refreezing into account when meltwater melts at the surface and penetrates through the snowpack. These routines have an effect on the runoff lag time and the amount of runoff (Mernild et al. 2008a). Not including retention/refreezing routines in SnowModel would lead to (1) an earlier outflow of runoff; and (2) an overestimation of the amount of runoff to the ocean. If no retention/refreezing routines were included in SnowModel, the initial seasonal runoff would occur up to 81 days before, and the Kangerlussuaq runoff would be overestimated up to ~65%. This value is below the previous values estimated for the Jakobshavn drainage area, averaging ~80% [*Mernild et al.*, 2009c], and above the entire GrIS of approximately ~25%, estimated by *Janssens and Huybrechts'* [2000] single-layer snowpack model [used, e.g., by *Hanna et al.*, 2002; 2005; 2008], and of 19–27% by *Mernild et al.* [2008a]. The SnowPack sub-model in SnowModel is similar to the one used by *Janssens and Huybrechts* [2000]; it does not calculate vertical temperature changes through the snowpack.

SnowModel also does not include the runoff routing and temporary storage aspects of the GrIS and proglacial landscape hydrology. These features clearly play important roles in controlling GrIS discharge hydrographs, and we are working to correct these deficiencies,. Water movement in and under a glacier is intrinsically complex and not well understood, because it involves the liquid phase (water) moving through the solid phase (ice) at the melting temperature, all while the ice is deformable and allowing englacier conduits to change size and shape. To improve our discharge simulations, in the short term, attempts will be made to (1) use SnowModel area-distributed runoff fluxes from the seasonal snowpack and the exposed glacier surface as inputs to hydrological routing models, for example, MIKE SHE (a spatially distributed, physically based hydrologic modeling system [*Refsgaard and Storm*, 1995]; and (2) include the GrIS drainage processes in SnowModel—the temporary seasonal storage buildup (delay) and release of runoff—in a submodel named IceHydro. Until then, the simple runoff 5-day (120-hour) running average routines presented herein will be used as a substitute.

Understanding the GrIS runoff and the hydrologic response is far from complete. Thus, the runoff observations from Kangerlussuaq have helped us to fill the gap in runoff exiting a part of the GrIS, and to understand the challenges we face by modeling GrIS runoff and its temporary seasonal storage and release of runoff. Efforts to model the GrIS mass balance, its dynamic processes, changes, internal drainage, and runoff with a holistic perspective, still suffer from important uncertainties and limitations. The limitations can be used as a guide to understand where long-term improvements should be made. How does the increasing volume of surface meltwater, due to increasing melt content, affect the GrIS dynamics, subglacier sliding processes, and the iceberg calving now and in a broader picture of global change? Further, how might the GrIS mass loss affect the arctic marine ecosystem, the freshwater contribution controlling the global eustatic sea level rise, and ocean salinity? These formidable questions promise to be at the frontier of arctic and climate-change science investigations in the coming years.

6. Summary and conclusion

This study presents the first runoff observations and daily and hourly runoff simulations from a large sector of the GrIS—the Kangerlussuaq drainage area—for the period 2006/07 and 2007/08. Our SnowModel runoff simulations have been verified against independent in situ observations (snow accumulation and runoff observations). This simulated GrIS series yielded useful insights into the present conditions and the inter-annual variability of Kangerlussuaq runoff. There is an acceptable degree of agreement between the simulated runoff and the recorded observations, both indicating a decreasing runoff from 2006/07 to 2007/08, strongly influenced by climate conditions and changes in storage. Further, the reduction in Kangerlussuaq runoff from 2006/07 to 2007/08 seems to follow the overall pattern in the satellite-derived GrIS surface melt for 2007 and 2008. Melting reduction in the broad GrIS perspective seems to occur simultaneously with runoff reduction from the Kangerlussuaq drainage area. The simulated runoff from Kangerlussuaq was on average ~1.9 km^3 and ~1.2 km^3 for 2006/07 and 2007/08, respectively. Understanding the GrIS runoff and the hydrologic response is far from complete. Thus, runoff observations from Kangerlussuaq have helped us to fill the gap in runoff exiting a part of the GrIS, and to understand the challenges we face by modeling the GrIS runoff and its temporarly seasonal storage (delay) and release of runoff due to dynamic processes and deformation of the internal drainage system.

Acknowledgment

We thank the Institute of Geography and Geology, University of Copenhagen, for the use of Kangerlussuaq runoff data; and the Institute for Marine and Atmospheric Research, Utrecht University, for the use of observed snow depth data and meteorological data from stations related to the K-transect on the Greenland Ice Sheet. We also thank the Cooperative Institute for Research in the Atmosphere, Colorado State University, for hosting the first author in February 2009. This work was supported by grants from the University of Alaska Presidential IPY Postdoctoral Foundation and from the Los Alamos National Laboratory, and carried out during the first author's postdoctoral program at the UAF and the LANL.

References

ACIA, 2005. Arctic Climate Impact Assessment. Cambridge University Press, 1042 p.

Allerup, P., H. Madsen, and F. Vejen, 1998. Estimating true precipitation in arctic areas. *Proc. Nordic Hydrological Conf.,* Helsinki, Finland, Nordic Hydrological Programme Rep. 44: 1–9.

Allerup, P., H. Madsen, and F. Vejen, 2000. Correction of precipitation based on off-site weather information. *Atmos. Res.,* 53: 231–250.

Anderson, E. A., 1976. A point energy balance model of a snow cover. NOAA Tech. Rep. NWS 19, 150 pp.

Bamber, J., S. Ekholm, and W. Krabill 2001. A new, high-resolution digital elevation model of Greenland fully validated with airborne laser altimeter data. J. Geophys. Res., 106(B4): 6733–6746.

Barnes, S. L., 1964. A technique for maximizing details in numerical weather map analysis. J. Appl. Meteor., 3: 396–409.

Barnes, S. L., 1973. Mesoscale objective analysis using weighted timeseries observations. NOAA Tech. Memo. ERL NSSL-62, National Severe Storms Laboratory, Norman, OK, 60 pp

Boggild, C. E., S. G. Warren, R. E. Brandt, and K. J. Brown 2006. Effects of dust and black carbon on albedo of the Greenland ablation zone. Abstract: American Geophysical Union, Fall Meeting 2006, abstract #U22A-05.

Born, E. W., and J. Böcher, 2001. *The Ecology of Greenland.* Ministry of Environment and Natural Resources, Nuuk, Greenland, 429 pp.

Box, J. E., D. H. Bromwich, B. A. Vennhuis, L.-S. Bai, J. C. Stroeve, J. C. Rogers, K. Steffen, T. Haren, and S.-H. Wang, 2006. Greenland ice sheet surface mass balance variability (1988-2004) from calibrated Polar MM5 output. Journal of Climate, 19: 2783–2800.

Broeke, M. van den, P. Smeets, J. Ettema, C. van der Veen, R. van de Wal, and J. Oerlemans 2008. partitioning of melt and meltwater fluxes in the ablation zone of the west Greenland ice sheet. The Cryosphere, 2: 179–189.

Bruland, O., G. E. Liston, J. Vonk, K. Sand, and A. Killingtveit, 2004. Modelling the snow distribution at two High-Arctic sites at Svalbard, Norway, and at a Sub-Arctic site in Central Norway. Nordic Hydrology, 35(3): 191–208.

Campbell, W. I., and Rasmussen, L. A. (1973). The production, flow and distribution of meltwater in a glacier treated as a porous medium. Hydrology of Glaciers (Proc. Cambridge Symp. Sept 1969). IAHS, 95, 11–27.

Dodson, R., and D. Marks, 1997. Daily air temperature interpolation at high spatial resolution over a large mountainous region. Climate Res., 8: 1–20.

Douville, H., J.-F. Royer, and J.-F. Mahfouf, 1995. A new snow paramerterization for the Meteo-France climate model. Part I: validation in stand-alone experiments. Climate Dynamics, 12: 21–35.

Dowdeswell, J. A., J. O. Hagen, H. Björnsson, A. F. Glazovsky, W. D. Harrison, P. Holmlund, J. Jania, R. M. Koerner, B. Lefauconnier, C. S. L. Ommanney, and R. H. Thomas, 1997. The Mass balance of Circum-Arctic Glaciers and Recent Climate Change. Quaternary Research 48, 1–4, no. QR971900: 1–14.

Essery, R. L. H., L. Li, and J. W. Pomeroy, 1999. A distributed model of blowing snow over complex terrain. *Hydrol. Processes,* 13: 2423–2438.

Ettema, J., M. van den Broeke, E. van Meijgaard, M. J. van de Berg, J. L. Bamber, J. E. Box, and R. C. Bales 2009. Higher surface mass balance of the Greenland ice sheet revealed by high-resolution climate modeling. Geophys. Res. Lett., 36, L12501, doi:10.1029/2009GL038110

Fettweis, X. 2007. Reconstruction of the 1979–2006 Greenland ice sheet surface mass balance using the regional climate model MAR. The Cryosphere, 1: 21–40.

Greene EM, Liston GE, Pielke RA. 1999. Simulation of above treeline snowdrift formation using a numerical snowtransport model. Cold Regions Science and Technology 30: 135–144.

Hanna, E., P. Huybrechts, and T. Mote, 2002. Surface mass balance of the Greenland ice sheet from climate-analysis data and accumulation/runoff models. Annals of Glaciology, 35: 67–72.

Hanna, E., P. Huybrechts, I. Janssens, J. Cappelen, K. Steffen, and A. Stephens, 2005. Runoff and mass balance of the Greenland ice sheet: 1958–2003. J. Geophys. Res., 110: 1–16.

Hanna, E., J. Box, and P. Huybrechts 2007. Greenland Ice Sheet mass balance. Arctic Report Card 2007, update to State of Arctic Report 2006, NOAA, available online at http://www.arctic.noaa.gov/reportcard/

Hanna, E., P. Huybrechts, K. Steffen, J. Cappelen, R. Huff., C. Shuman, T. Irvine-Fynn, S. Wise, and M. Griffiths, 2008. Increased Runoff from melt from the Greenland Ice Sheet: A response to Global Warming. Journal of Climate, 21: 331–341.

Hanna, E., J. Cappelen, X. Fettweis, P. Huybrechts, A. Luckman, M. H. Ribergaard 2009. Hydrologic response of the Greenland Ice sheet: the role of oceanographic warming. Hydrological Processes, 23: 7–30.

Hasholt, B. and Mernild S. H. 2009. Runoff and Sediment Transport Observations from the Greenland Ice Sheet, Kangerlussuaq, West Greenland. 17th International Northern Research Basins Symposium and Workshop, pp. 1-8.

Hiemstra, C. A., G. E. Liston, and W. A. Reiners, 2002. Snow Redistribution by Wind and Interactions with Vegetation at Upper Treeline in the Medicine Bow Mountains, Wyoming. Arctic, Antarctic, and Alpine Research, 34: 262–273.

Hiemstra, C. A., G. E. Liston, and W. A. Reiners, 2006. Observing, modelling, and validating snow redistribution by wind in a Wyoming upper treeline landscape. Ecological Modelling, 197: 35–51.

Hock, R., and C. Hoetzli, 1997. Areal melt and discharge modelling of Storglacia¨ren, Sweden. International Symposium on Changing Glaciers, Fjærland, Norway, 24–27 June. Annal. Glaciol., 24, 211–216.

IPCC, 2007: Summary for Poicymakers. In: Climate Change 2007. The Physical Science Basis. Contribution of Working Group I to the Fourth Assessment Report of the Intergovernmental Panel on Climate Change [Solomon, S., D. Qin, M. Manning, Z. Chen, M. Marquis, K.B. Averyt, M.Tignor and H.L. Miller (eds.)]. Cambridge University Press, Cambridge, United Kingdom and New York, USA.

Iziomon, M. G., H. Mayer, and A. Matzarakis, 2003. Downward atmospheric longwave irradiance under clear and cloudy skies: Measurement and parameterization. J. Atmos. Sol.-Terr. Phys., 65: 1107–1116.

Janssens, I., and P. Huybrechts, 2000. The treatment of meltwater retention in mass-balance parameterisation of the Greenland Ice Sheet. *Ann. Glaciol.,* 31: 133–140.

Jansson, P., R. Hock, and T. Schneider, 2003. The concept of glacier storage: a review. Journal of Hydrology 282: 116–129.

Johannessen, O. M., K. Khvorostovsky, M. W. Miles, and L. P. Bobylev, 2005. Recent ice sheet growth in the interior of Greenland, Sciencexpress, 1013–1016, doi:10.1126/science.1115356.

Koch, S. E., M. DesJardins, and P. J. Kocin, 1983. An interactive Barnes objective map analysis scheme for use with satellite and conventional data. J. Climate Appl. Meteor., 22: 1487–1503.

Krabill, W. E., and Coauthors, 2000. Greenland ice sheet: Highelevation balance and peripheral thinning. *Science,* 289: 428–430.

Krabill W., E. Hanna, P. Huybrechts, W. Abdalati, J. Cappelen, B. Csatho, E. Frederick, S. Manizade, C. Martin, J. Sonntag, R. Swift, R. Thomas, and J. Yunge, 2004. Greenland Ice Sheet: Increased coastal thinning, Geophys. Res. Lett., 31, L24402, doi:10.1029/2004GL021533.

Kunkel, K. E., 1989. Simple procedures for extrapolation of humidity variables in the mountains western United States. J. Climate, 2: 656–669.

Lemke, P., J. Ren, R. B. Alley, I. Allison, J. Carrasco, G. Flato, Y. Fujii, G. Kaser, P. Mote, R. H. Thomas, and T. Zhang, 2007. Observations: Changes in Snow, Ice and Frozen Ground, in: Climate Change 2007: The Physical Science Basis, Contribution of Working Group I to the Fourth Assessment Report of the Intergovernmental Panel on Climate Change, edited by: Solomon, S., Qin, D., Manning, M., Chen, Z., Marquis, M., Averyt, K. B., Tignor M., and Miller, H. L., Cambridge University Press, United Kingdom and New York, USA.

Liston G. E. 1995. Local Advection of Momentum, Heat, and Moisture during the Melt of Patchy Snow Covers. *Journal of Applied Meteorology* 34(7): 1705–1715.

Liston, G. E., and D. K. Hall, 1995. An energy-balance model of lake-ice evolution. J. Glaciol., 41: 373–382.

Liston, G. E., and M. Sturm, 1998. A snow-transport model for complex terrain. J. Glaciol. 44: 498–516.

Liston, G. E., and M. Sturm, 2002. Winter Precipitation Patterns in Arctic Alaska Determined from a Blowing-Snow Model and Snow-Depth Observations. Journal of hydrometeorology, vol. 3: 646–659.

Liston, G. E., and M. Sturm, 2004. The role of winter sublimation in the Arctic moisture budget. Nordic Hydrology, 35(4): 325–334.

Liston, G. E., and J.-G. Winther, 2005. Antarctic surface and subsurface snow and ice melt fluxes. J. Climate, 18(10): 1469–1481.

Liston, G. E., and K. Elder, 2006a. A distributed snow-evolution modeling system (SnowModel). Journal of Hydrometeorology, 7: 1259–1276.

Liston, G. E., and K. Elder, 2006b. A meteorological distribution system for high resolution terrestrial modeling (MicroMet). Jounal of Hydrometeorology, 7: 217–234.

Liston, G. E., and C. A. Hiemstra, 2008. A simple data assimilation system for complex snow distributions (SnowAssim). J. Hydrometeorology, 9: 989–1004.

Liston, G. E., J.-G. Winther, O. Bruland, H. Elvehøy, and K. Sand, 1999. Below surface ice melt on the coastal Antarctic ice sheet. J. Glaciol., 45(150): 273–285.

Liston, G. E., J. P. McFadden, M. Sturm, and R. A. Pielke Sr., 2002: Modeled changes in arctic tundra snow, energy, and moisture fluxes due to increased shrubs. *Global Change Biol.,* **8,** 17–32.

Liston, G. E., R. B. Haehnel, M. Sturm, C. A. Hiemstra, S. Berezovskaya, and R. D. Tabler, 2007. Simulating complex snow distributions in windy environments using SnowTran-3D. Journal of Glaciology, 53: 241–256.

Liston, G. E., C. A. Hiemstra, K. Elder, and D. W. Cline, 2008. Meso-cell study area (MSA) snow distributions for the Cold Land Processes Experiment (CLPX). J. Hydrometeorology, 9: 957–976.

Mernild, S. H. and G. E. Liston, 2009. The influence of air temperature inversion on snow melt and glacier surface mass-balance simulations, SW Ammassalik Island, SE Greenland. In review *Journal of Applied Meteorology and Climate*.

Mernild, S. H., G. E. Liston, B. Hasholt, and N. T. Knudsen, 2006a. Snow distribution and melt modeling for Mittivakkat Glacier, Ammassalik Island, SE Greenland. *J. Hydrometeor.*, 7: 808–824.

Mernild, S. H., B. Hasholt, and G. E. Liston, 2006b. Water flow through Mittivakkat Glacier, Ammassalik Island, SE Greenland. Danish Journal of Geography, 106(1): 25–43.

Mernild, S. H., G. E. Liston, and B. Hasholt, 2007. Snow-Distribution and Melt Modeling for Glaciers in Zackenberg River Drainage Basin, NE Greenland. Hydrological Processes. 21: 3249–3263. DOI: 10.1002/hyp.6500.

Mernild, S. H., G. E. Liston, C. A., Hiemstra, and K. Steffen, 2008a. Surface Melt Area and Water Balance Modeling on the Greenland Ice Sheet 1995–2005. Journal of Hydrometeorology, 9(6): 1191–1211. doi: 10.1175/2008JHM957.1

Mernild, S. H., G. E. Liston, and B. Hasholt, 2008b. East Greenland freshwater runoff to the Greenland-Iceland-Norwegian Seas 1999–2004 and 2071–2100. Hydrological Processes, 22: 4571–4586. DOI: 10.1002/hyp.7061.

Mernild, S. H. and B. Hasholt 2009. Observed runoff, jökulhlaups, and suspended sediment load from the Greenland Ice Sheet at Kangerlussuaq, West Greenland, for 2007 and 2008. Accepted *Journal of Glaciology*.

Mernild, S. H., B. Hasholt, and G. E. Liston, 2008c. Climatic control on river discharge simulations, Zackenberg River Drainage basin, NE Greenland. Hydrological Processes, 22: 1932–1948. DOI: 10.1002/hyp.6777.

Mernild, S. H., Hasholt, B., Kane, D. L., and Tidwell, A. C. 2008d. Jökulhlaup Observed at Greenland Ice Sheet. *Eos Trans. AGU*, 99(35): 321–322.

Mernild, S. H., G. E. Liston, C. A. Hiemstra, and K. Steffen, 2009a. Record 2007 Greenland Ice Sheet surface melt-extent and runoff. Eos Trans. AGU.

Mernild, S. H., G. E. Liston, C. A. Hiemstra, K. Steffen, E. Hanna, and J. H. Christensen, 2009b. Greenland Ice Sheet surface mass-balance modeling and freshwater flux for 2007, and in a 1995–2007 perspective. Hydrological Processes, DOI: 10.1002/hyp.7354

Mernild, S. H., G. E. Liston, K. Steffen, and P. Chylek 2009c. Meltwater flux and runoff modeling in the ablation area of the Jakobshavn Isbræ, West Greenland. In review *Journal of Glaciology*.

Nick, F. M, A. Vieli, I. M. Howat, and I. Joughin, 2009. Large-scale changes in Greenland outlet glacier dynamics triggred at the terminus. Nature Geoscience, 2: 110–114.

Parizek, B. R. and Alley, R. B. 2004. Implications of increased Greenland surface melt under global-warming scenarios: Ice-sheet simulations, Quat. Sci. Rev. 23: 1013–1027.

Pielke, R. A., Sr., 2002. Mesoscale Meteorological Modeling. Academic Press, 676 pp.

Pomeroy, J. W., and R. L. H. Essery, 1999. Turbulent fluxes during blowing snow: Field test of model sublimation predictions. *Hydrol. Processes,* 13: 2963–2975.

Prasad, R., D. G. Tarboton, G. E. Liston, C. H. Luce, and M. S. Seyfried, 2001. Testing a blowing snow model against distributed snow measurements at Upper Sheep Creek. Water Resour. Res., 37: 1341–1357.

Refsgaard JC, Storm B. 1995. MIKE SHE. In Computer Models of Watershed Hydrology, Singh VJ (ed.). Water Resources Publication: Littleton, CO; 809–846.

Richardson, K., W. Steffen, H. Schellnhuber, J. Alcamo, T. Barker, D. Kammen, R. Leemans, D. Liverman, M. Munasinghe, B. Osman-Elasha, N. Stern, O. Waever (2009), Climate Change: Global Risks, Challenges and Decisions, Synthesis Report, Copenhagen, 10–12 March, University of Copenhagen, pp. 39.

Ryan, B. C., 1977. A mathematical model for diagnosis and prediction of surface winds in mountains terrain. J. Appl. Meteor., 16: 1547–1564.

Scambos, T. and T. Haran 2002. An image-enhanced DEM of the Greenland Ice Sheet. Annals of Glaciology, 34: 291–298.

Serreze, M. C. and R. G. Barry, 2005. The Arctic Climate System. Cambridge Atmospheric and Space Science Series: Cambridge; p. 424.

Steffen, K. and J. Box, 2001. Surface climatology of the Greenland Ice Sheet: Greenland climate network 1995–1999. Journal of Geophysical Research, 106(24): 33951–33964.

Stenborg, T. (1970): Delay of runoff from a glacier basin. Geografiske Annaler 52A: 1–30.

Strack, J. E., G. E. Liston, R. A. Pielke Sr. 2004. Modeling Snow Depth for Improved Simulation of Snow-Vegetation-Atmosphere Interactions. Journal of Hydrometeorology, 5: 723–734.

Thornton, P. E., S. W. Running, and M. A. White, 1997. Generating surfaces of daily meteorological variables over large regions of complex terrain. J. Hydrol., 190: 214–251.

van de Wal, R. S. W., W. Greuell, M. R. van den Broeke, C. H. Reijmer, and J. Oerlemans 2005. Surface mass-balance observations and automatic weather station data along a transect near Kangerlussuaq, West Greenland. Annals of Glaciology, 42: 311–316.

van de Wal, R. S. W., W. Boot, M. R. van den Broeke, C. J. P. P. Smeets, C. H. Reijmer, J. J. A. Donker, and J. Oerlemans, 2008. Large and Rapid Melt-Induced Velocity Change in the Ablation Zone of the Greenland Ice Sheet. Science 321, DOI: 10.1126/science.1158540, 111–113.

van den Broeke, M., P. Smeets, J. Ettema, and P. K. Munneke 2008a. Surface radiation balance in the ablation zone of the west Greenland ice sheet. *J. Goephys. Res.*, 113,D13105, doi:10.1029/2007/JD009283.

van den Broeke, M., P. Smeets, J. Ettema, C. van der Veen, R. van de Wal, and J. Oerlemans 2008b. Partitioning of melt energy and meltwater fluxes in the ablation zone of the west Greenland ice sheet. *The Cryosphere*, 2: 179–189.

van den Broeke, M., P. Smeets, and J. Ettema 2008c. Surface layer climate and turbulent exchange in the ablation zone of the west Greenland ice sheet. International Journal of Climatology. DOI: 10.1002/joc.1815.

Walcek, C. J., 1994. Cloud cover and its relationship to relative humidity during a spring midlatitude cyclone. Mon. Wea. Rev., 122: 1021–1035.

Yang, D., S. Ishida, B. E. Goodison, and T. Gunther, 1999. Bias correction of precipitation data for Greenland. Journal of Geophysical Research-Atmospheres, 104, (D6): 6171–6181.

Zwally, J. H., W. Abdalati, T. Herring, K. Larson, J. Saba, and K. Steffen, 2002. Surface melt-induced acceleration of Greenland ice-sheet flow. Science, 297: 218–222.

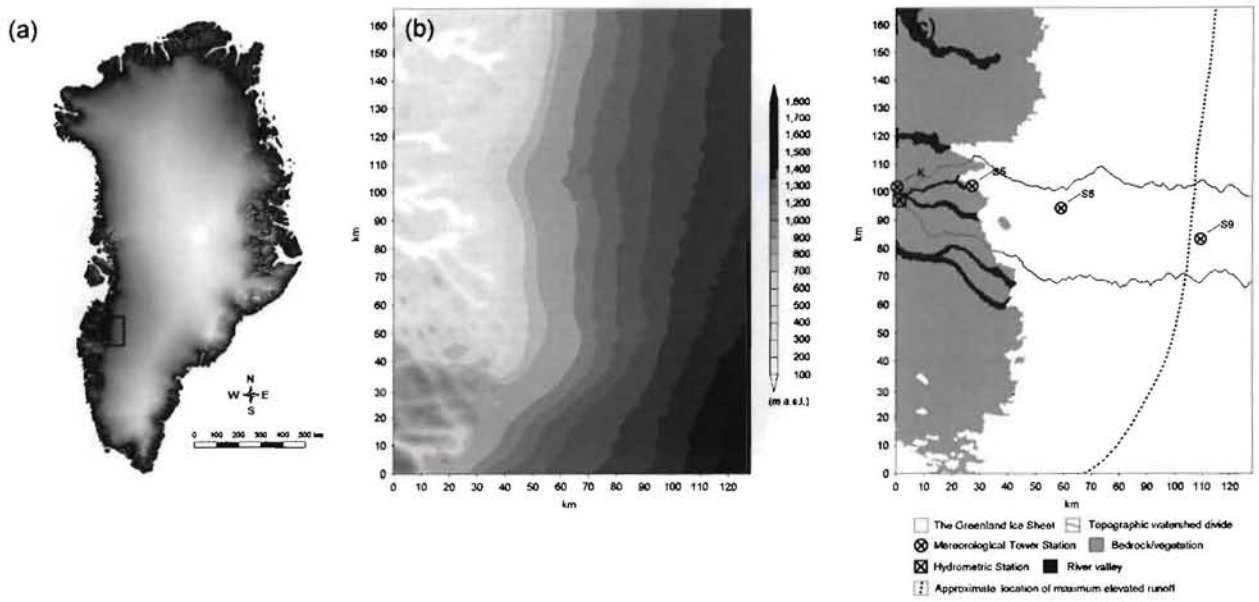

Figure 1: (a) The Kangerlussuaq region in western Greenland, including the simulation area (21,248 km^2); (b) simulation area with topography (gray shades, 100-m contour interval); and (c) simulation area land cover characteristics including the four meteorological stations: Station K (50 m a.s.l.), S5 (490 m a.s.l.), S6 (1,020 m a.s.l.), and S9 (1,520 m a.s.l.), the hydrometric station at the catchment outlet, the approximate location of maximum elevated runoff, and the surface watershed divide. The surface watershed divide is estimated based on RiverTools.

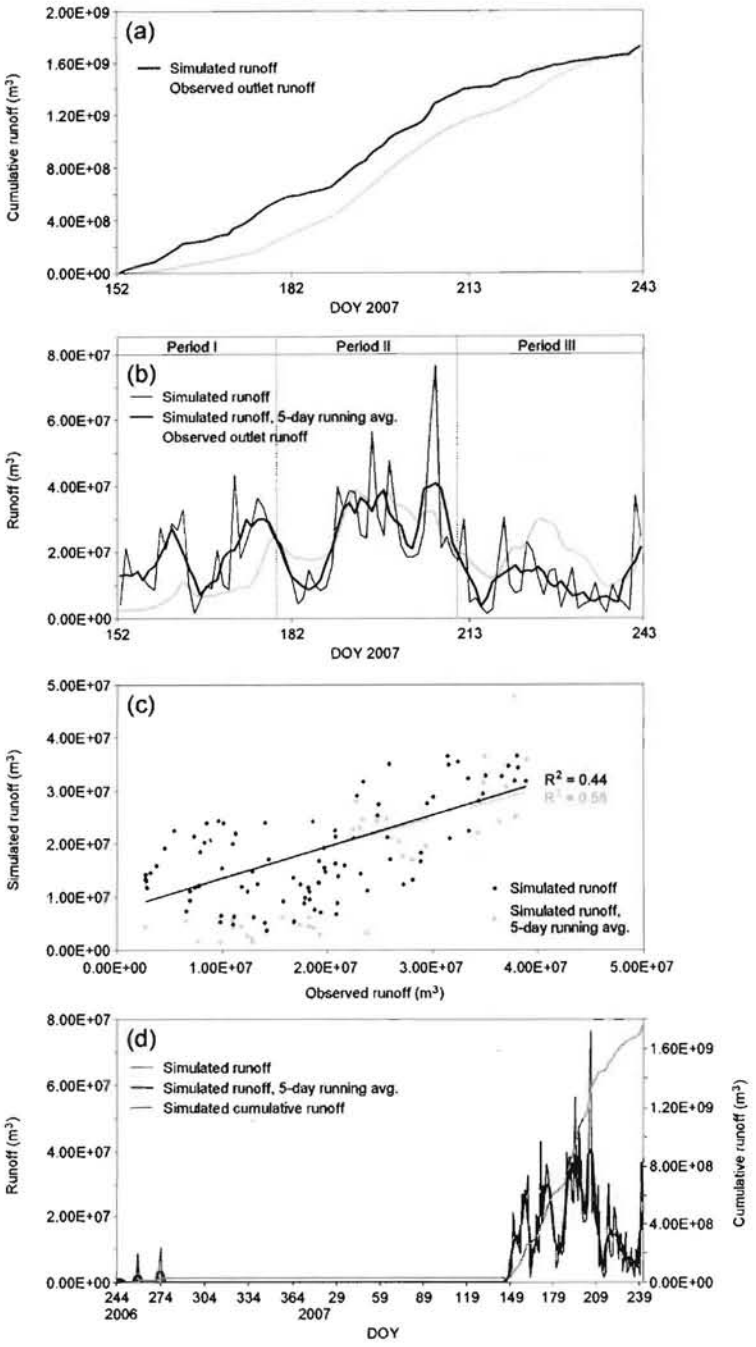

Figure 2: Daily observed and simulated runoff at the GrIS Kangerlussuaq drainage area for the 2006/07 runoff season: (a) cumulative observed and simulated runoff from 1 June (DOY 152) through 31 August (DOY 243); (b) observed, simulated, and simulated 5-day running average runoff; (c) a comparison (linear regression) between observed and modeled runoff, and observed and simulated 5-day running average runoff; and (d) simulated runoff, including cumulative runoff from 1 September (DOY 244) to 31 August.

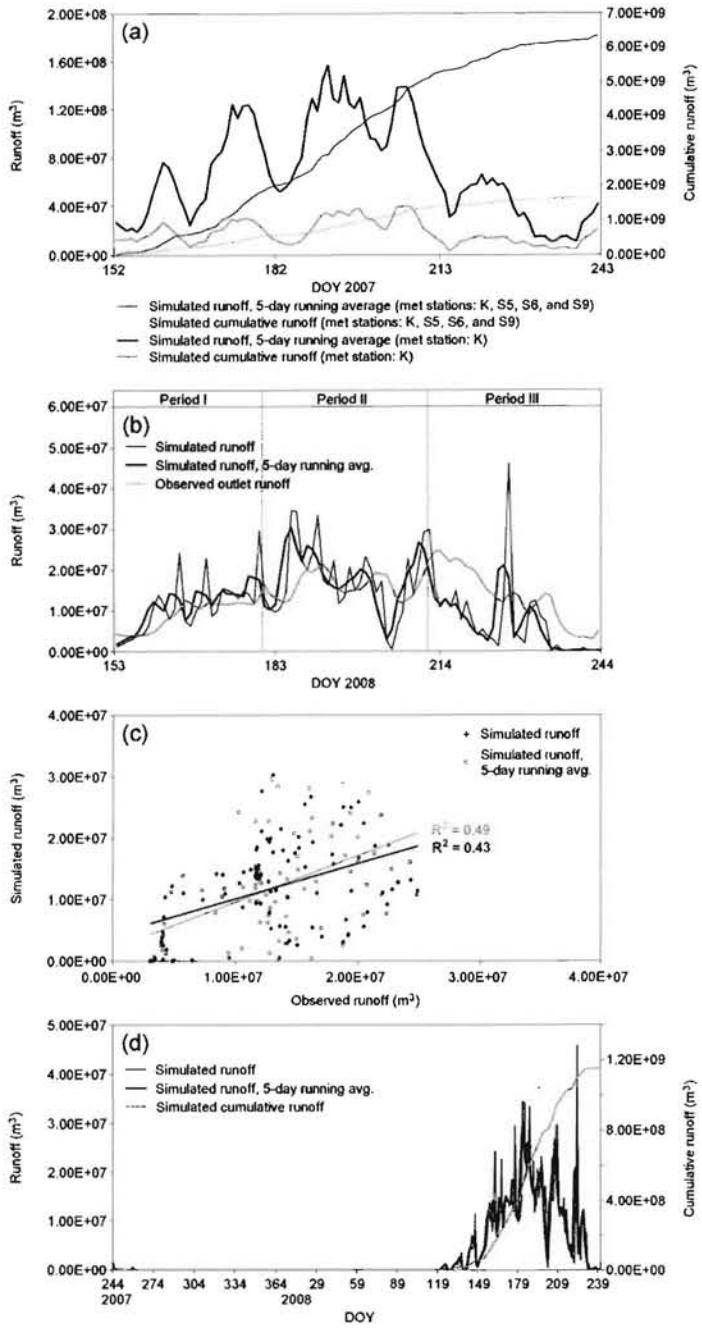

Figure 3: Daily observed and simulated runoff at the GrIS Kangerlussuaq drainage area for the 2006/07 and 2007/08 runoff seasons: (a) test simulation of the 2007 runoff (1 June through 31 August) based on meteorological data from all four stations, and from the Kangerlussuaq DMI station itself; (b) observed, simulated, and simulated 5-day running average runoff; (c) a comparison (linear regression) between observed and modeled runoff, and observed and simulated 5-day running average runoff; and (d) simulated runoff, including cumulative runoff from 1 September (DOY 244) to 31 August.

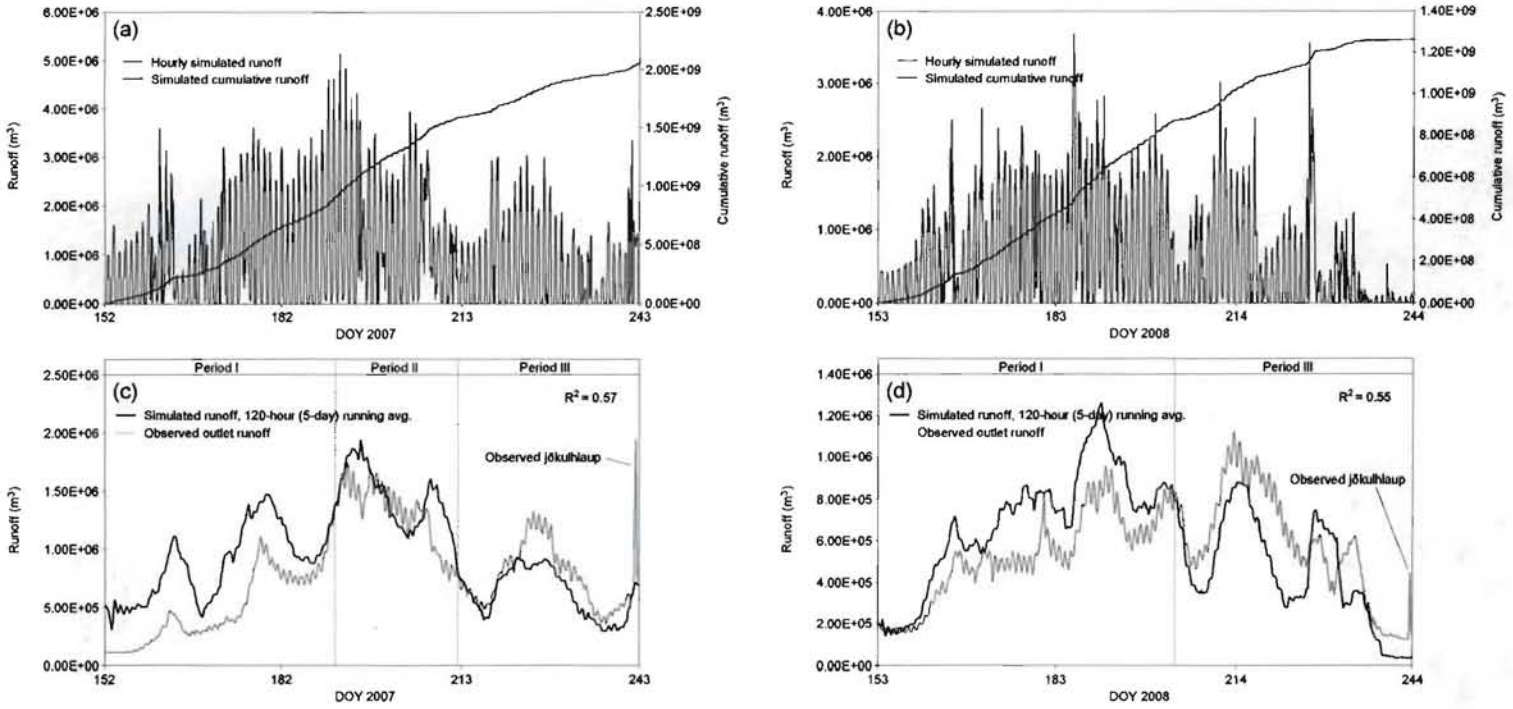

Figure 4: Hourly observed and simulated runoff and cumulative runoff at the GrIS Kangerlussuaq drainage area for the 2006/07 and 2007/08 runoff seasons: (a) simulated runoff from 1 June through 31 August 2007; (b) simulated runoff from 1 June through 31 August 2008; (c) observed and simulated 5-day running average runoff 1 June through 31 August 2007, including observed jökulhlaup 31 August (DOY 243); and (d) observed and simulated 5-day running average runoff 1 June through 31 August 2008, including observed jökulhlaup 31 August (DOY 244).

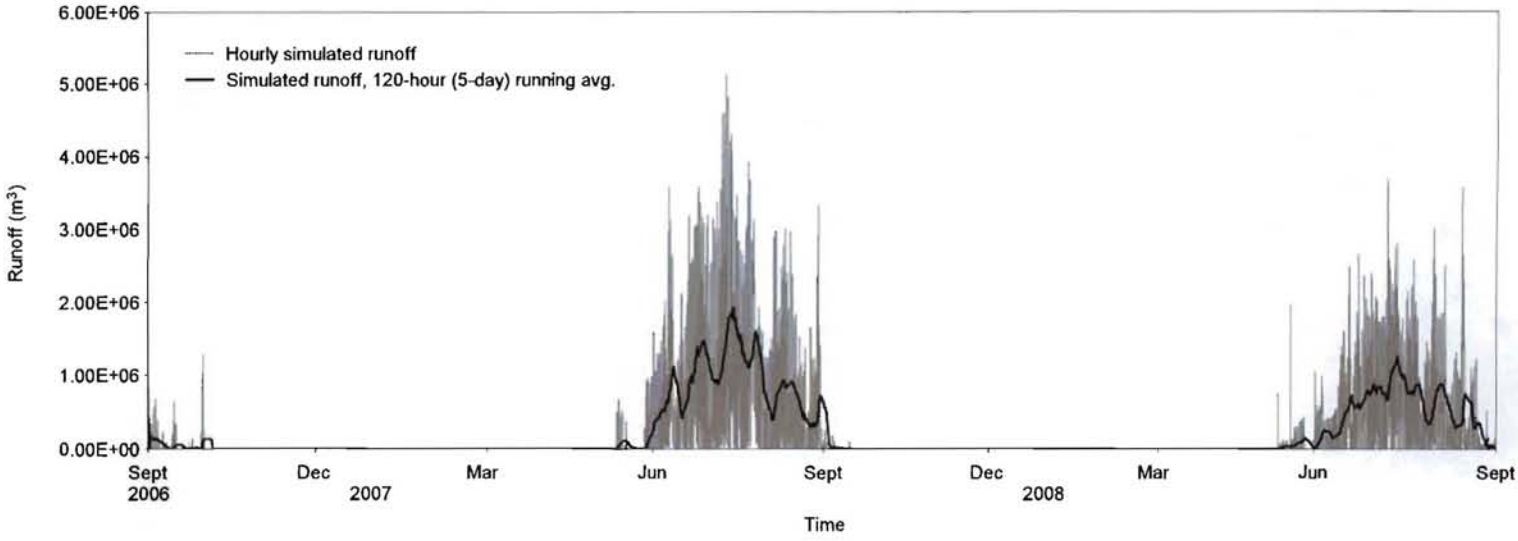

Figure 5: Hourly simulated runoff at the GrIS Kangerlussuaq drainage area for the 2006/07 and 2007/08 runoff seasons.

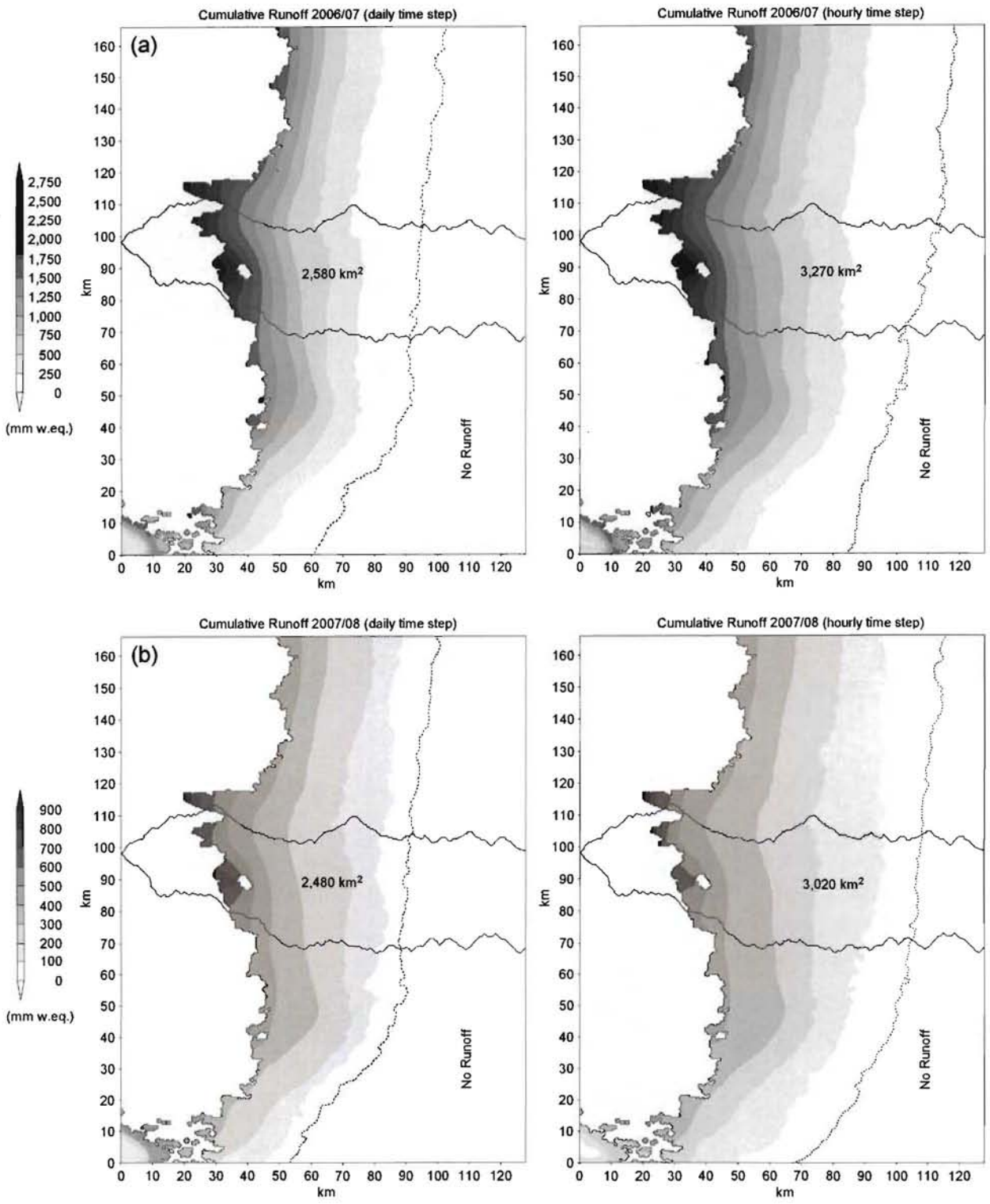

Figure 6: Spatial daily and hourly simulated runoff distribution for the 2006/07 and 2007/08 runoff seasons at the GrIS Kangerlussuaq drainage area, including watershed divide and catchment runoff area (used for calculation of the specific runoff).

Table 1: Meteorological input data for the Kangerlussuaq SnowModel simulations. Meteorological station data on the GrIS (S5, S6, and S9) were provided by the Utrecht University, and coastal meteorological station data (K; Kangerlussuaq) by the Danish Meteorological Institute (DMI). For further information about the S-stations, see, e.g., *van den Broeke et al.* [2008].

Meteorological station name	Location	Grid	Data time period for runoff simulations	Altitude (m a.s.l.)	Parameters
K	Town Kangerlussuaq	67°01′N, 50°42′W	1 Sep 2006 – 31 Aug 2008	50	Air temperature, relative humidity, wind speed, wind direction, and corrected precipitation
S5	Ice Sheet	67°06′N, 50°07′W	1 Sep 2006 – 31 Aug 2007	490	Air temperature and wind speed
S6	Ice Sheet	67°05′N, 49°23W	1 Sep 2006 – 31 Aug 2007	1,020	Air temperature and wind speed
S9	Ice Sheet	67°03′′N, 48°14′W	1 Sep 2006 – 31 Aug 2007	1,520	Air temperature and wind speed

Table 2: Mean monthly air temperature lapse rates for the Kangerlussuaq area and on the GrIS, based on data from the transect between the meteorological stations S5 (490 m a.s.l.), S6 (1,020 m a.s.l.), and S9 (1,520 m a.s.l.) (from September 2003 through August 2007). See Figure 1b for meteorological station locations and Table 2 for station information.

	Jan	Feb	Mar	Apr	May	Jun	Jul	Aug	Sept	Oct	Nov	Dec	Avg
The GrIS area based on stations: S5, S6, and S9 ($^{\circ}C\ km^{-1}$)	-6.3	-7.0	-7.3	-5.6	-7.5	-5.2	-4.6	-4.8	-7.8	-8.6	-8.1	-7.4	-6.7

Table 3: User-defined constants used in the SnowModel simulations (see *Liston and Sturm* [1998] for parameter definitions).

Symbol	Value	Parameter
C_v		Vegetation snow-holding depth (equal surface roughness length) (m)
	0.50	- Barren bedrock/vegetation
	0.50	- River valley
	0.01	- Ice/snow
F	500.0	Snow equilibrium fetch distance (m)
U_{*t}	0.25	Threshold wind-shear velocity (m s^{-1})
Z_0	0.01	Snow surface roughness length (m)
dt	1	Time step (daily and hourly)
$dx = dy$		Grid cell increment (km)
	0.5	- Greenland Ice Sheet Kangerlussuaq simulation area
α		Surface albedo
	0.5–0.8	- Snow (variable snow albedo according to surface snow characteristics)
	0.4	- Ice
ρ		Surface density (kg m^{-3})
	280	- Snow
	910	- Ice
ρ_s	550	Saturated snow density (kg m^{-3})

Table 4: Observed and modeled snow depth for Station S9 at the end of winter (31 May; recognized as the end of the accumulation period) (for station specifications, see Figure 1 and Table 2).

Year	Observed end-of-winter (31 May) snow depth at Station S9 (mm) [*van den Broeke et al.*, 2008b]	Modeled end-of winter (31 May) snow depth at Station S9 based on precipitation data from Station K in Kangerlussuaq (mm)	Difference in observed and modeled end-of winter (31 May) snow depth at Station S9 based on precipitation data from the Station K in Kangerlussuaq (mm and %)	Modeled end-of winter (31 may) snow depth at Station S9, based on iterative precipitation adjustment routines described in *Mernild et al.* [2006a] and *Liston and Hiemstra* [2008] (mm)
2003/04	830	1,450	620	820
2004/05	1,090	1,430	340	1,090
2005/06	870	1,160	290	870
2006/07	730	1.070	340	730
Average and standard deviation	880(±150)	1,280(±190)	400(±150) ~50%	880(±150)

Table 5: Observed and SnowModel daily simulated discharge and cumulative runoff from the GrIS Kangerlussuaq drainage area for 2006/07 and 2007/08. Simulations are based on meteorological data from a combination of different stations.

	Period	Meteorological stations used for simulation	Daily average and maximum discharge ($m^3 s^{-1}$)	Maximum daily difference in observed and simulated runoff (m^3)	Cumulative runoff (m^3)	Difference in observed and simulated cumulative runoff (%)
Observed discharge and runoff at the catchment outlet	June through August, 2007	-----	216.2 449.1	-----	1.719×10^9	-----
Simulated discharge and runoff		K, S5, S6, and S9	423.2 1,717.1	1.168×10^8	3.336×10^9	~90
Adjusted simulated discharge and runoff		K, S5, S6, and S9	216.2 884.7	0.449×10^8	1.718×10^9	<1
Adjusted simulated 5-day running average discharge and runoff		K, S5, S6, and S9	215.8 472.0	0.207×10^8	1.718×10^9	<1
Simulated 5-day running average discharge and runoff		K	796.3 1,813.5	1.945×10^8	6.338×10^9	~270
Adjusted simulated 5-day running average discharge and runoff	September 2006 through August 2007	K, S5, S6, and S9	144.8 472.0	-----	1.757×10^9	-----
Observed discharge and runoff at the catchment outlet	June through August, 2008	-----	152.4 288.5	-----	1.211×10^9	-----
Adjusted simulated discharge and runoff		K	138.6 531.7	0.321×10^8	1.101×10^9	~10
Adjusted simulated 5-day running average discharge and runoff		K	138.6 312.9	0.131×10^8	1.101×10^9	~10
Adjusted simulated 5-day running average discharge and runoff	September 2007 through August 2008	K	92.1 312.9	-----	1.154×10^9	-----

Table 6: SnowModel daily and hourly simulated cumulative runoff from the GrIS Kangerlussuaq drainage area for 2006/07 and 2007/08.

	Period	Meteorological stations used for simulation	Cumulative runoff (m^3)	Part of runoff originating from the GrIS glacier ice (m^3 and %)
Daily simulated cumulative runoff	June through August, 2007	K, S5, S6, and S9	1.718×10^9	-----
Hourly simulated cumulative runoff		K, S5, S6, and S9	1.955×10^9	-----
Difference in hourly and daily simulated cumulative runoff (m^3 and %)		-----	0.237×10^9 ~14%	-----
Daily simulated cumulative runoff, 5-day running average	September 2006 through August 2007	K, S5, S6, and S9	1.757×10^9	1.011×10^9 ~58%
Hourly simulated cumulative runoff, 5-day (120 hour) running average		K, S5, S6, and S9	2.055×10^9	1.326×10^9 ~64%
Difference in hourly and daily simulated cumulative runoff (m^3 and %)		-----	0.298×10^9 ~17%	-----
Daily simulated cumulative runoff	June through August, 2008	K	1.101×10^9	-----
Hourly simulated cumulative runoff		K	1.190×10^9	-----
Difference in hourly and daily simulated cumulative runoff (m^3 and %)		-----	0.089×10^9 ~6%	-----
Daily simulated cumulative runoff, 5-day running average	September 2007 through August 2008	K	1.154×10^9	0.627×10^9 ~54%
Hourly simulated cumulative runoff, 5-day (120 hour) running average		K	1.263×10^9	0.694×10^9 ~55%
Difference in hourly and daily simulated cumulative runoff (m^3 and %)		-----	0.109×10^9 ~9%	-----